Thermoplastic Apparent Interpenetrating Polymer Networks of Polyurethane and Styrene/Acrylic Acid Block Copolymer: Structure–Property Relationships

A. Kanapitsas,[1,2] E. Lebedev,[3] O. Slisenko,[3] O. Grigoryeva,[3] P. Pissis[1]

[1]*National Technical University of Athens, Department of Physics, Zografou Campus, 15780 Athens, Greece*
[2]*Technological Educational Institute of Lamia, Electronics Department, Old National Road Lamia–Athens, 35100 Lamia, Greece*
[3]*Institute of Macromolecular Chemistry, National Academy of Sciences of Ukraine, 02160 Kyiv, Ukraine*

Received 20 June 2005; accepted 6 September 2005
DOI 10.1002/app.23093
Published online in Wiley InterScience (www.interscience.wiley.com).

ABSTRACT: Thermoplastic apparent interpenetrating polymer networks (t-AIPNs) of crystallizable polyurethane (CPU) and a styrene/acrylic acid block copolymer (S-*b*-AA, acid form) of several compositions were prepared by casting from a common solvent. A variety of experimental techniques, including size exclusion chromatography (SEC), differential scanning calorimetry (DSC), thermogravimetric analysis (TGA), dynamic mechanical analysis (DMA), broadband dielectric relaxation spectroscopy (DRS), thermally stimulated depolarization currents (TSDC), and density measurements were employed to investigate structure–property relationships of the t-AIPNs. Special attention was paid to the investigation of molecular dynamics of the CPU component in the t-AIPNs, by combination of the dielectric DRS and TSDC techniques, as well as from the methodological point of view, to the prospects of morphological characterization by broadband DRS. The results show that the CPU/S-*b*-AA t-AIPNs studied can be considered as multiphase systems having at least two amorphous and one crystalline phases, as well as regions of mixed compositions. Their properties are determined by the heterogeneity of the individual components, as well as by the heterogeneity caused by the thermodynamic incompatibility of these components. The degree of incompatibility is determined, to a large extent, by the intermolecular hydrogen bonding between the functional groups of the CPU and the S-*b*-AA components (ester groups and COOH-groups, respectively), which is more effective on addition of small amounts of either of the components. © 2006 Wiley Periodicals, Inc. J Appl Polym Sci 101: 1021–1035, 2006

Key words: thermoplastic apparent interpenetrating polymer networks; mixed microphase; H-bonding; microheterogeneity; molecular dynamics

INTRODUCTION

Segmented polyurethanes, PUs, are typical representatives of linear block copolymers of the type $(A–B)_n$ and an important class of thermoplastic elastomers. The versatile physical properties of PUs are generally attributed to their microphase-separated structure, arising from the thermodynamic incompatibility of hard segments (HS) and soft segments (SS) and consisting, in general, of HS domains embedded within a SS matrix, the interphase being ill-defined.[1] By varying the fraction of HS, thermoplastics with a wide range of viscoelastic properties can be produced. However, owing to low rigidity and high-thermal expansion, the mechanical performance of PUs is inappropriate for structural applications. This drawback is typically overcome by addition of a second, proper polymer component, very often in the form of interpenetrating polymer networks (IPNs). Thus, IPNs of PUs with various types of polymers have been widely investigated and used as industrial materials.[2–5]

IPNs may be defined as binary polymer systems, in which at least one component is chemically crosslinked (as a rule, by covalent bonds) to avoid the incipient phase separation.[6–8] They provide the possibility of effectively producing advanced multicomponent polymeric systems with new property profiles. In contrast to true IPNs, in thermoplastic IPNs, t-IPNs, the components are crosslinked by physical, instead of chemical, bonds, like ionic and hydrogen bonds, as well as microcrystallites playing the role of effective crosslinks.[8–11] Thus, t-IPNs are intermediate between true IPNs and blends of linear polymers, as they behave like the former at relatively low temperatures and like the latter at high temperatures.

In previous work, we investigated the structure–property relationships in t-IPNs prepared from a crystallizable polyurethane (CPU) and a random copolymer of styrene/acrylic acid (S/AA).[10–14] These mix-

Correspondence to: P. Pissis (ppissis@central.ntua.gr).
Contract grant sponsor: European Social Fund and National Resources (EPEAEK II)-PYTHAGORAS; Contract grant sponsor: Greek State Scholarships Foundation (IKY).

tures were called thermoplastic apparent IPNs, t-AIPNs, because S/AA was used in the acid form and not in the salt form. With structure–property relationships, we mean the complex of relationships between composition, processing, structure/morphology, dynamics and properties/performance of the materials under investigation. A better understanding of these relationships is essential for optimizing composition and processing of materials to meet specific end-use requirements. Both t-AIPNs prepared by melt mixing of the components[13,14] and by casting from a common solvent[10,12] were investigated. The results by a variety of experimental techniques showed that the t-AIPNs were microheterogeneous systems with contributions to microheterogeneity from both the heterogeneity of the individual polymers and the thermodynamic incompatibility of the components. On the other hand, deviations from additivity and significant changes of several properties on addition of small amounts of either of the components indicated partial miscibility, explained by the formation of hydrogen bonds between functional groups of the two components.[12,13]

In the work presented here, we continue the investigation of t-AIPNs based on CPU and S/AA copolymer. The random copolymer has been replaced here by a block copolymer (S-*b*-AA) and the molar fraction of AA in the copolymer was significantly reduced from 28 to 10%. We expect that interaction between the two IPN components, mostly hydrogen bonding between the COOH— groups of AA in S-*b*-AA and the ester groups of the flexible CPU blocks,[13] and, thus, partial miscibility, will be affected by these changes. Moreover, individual properties of the two components of the block copolymer may now show up in the final t-AIPNs. Finally, the amount of AA in the copolymer was reduced having in mind, as a next step of this work, the preparation, by partial neutralization of AA, of the salt form of these IPNS, i.e., true t-IPNs, where aggregation in clusters should be avoided.[15]

A variety of experimental techniques, including size exclusion chromatography (SEC), differential scanning calorimetry (DSC), thermogravimetric analysis (TGA), dynamic mechanical analysis (DMA), broadband dielectric relaxation spectroscopy (DRS), thermally stimulated depolarization currents (TSDC) measurements, and density measurements were employed in this work, and the results are discussed in terms of morphology, molecular mobility, and properties of the t-AIPNs under investigation. Special attention was paid to the investigation of molecular dynamics of the CPU component in the t-AIPNs, by combination of the dielectric DRS and TSDC techniques, as well as, from the methodological point of view, to the prospects of morphological characterization by broadband DRS.

EXPERIMENTAL

Materials

The crystallizable polyurethane (CPU) was prepared by the reaction (3 h at 75°C) of toluene diisocyanate, TDI (mixture of 2,4- and 2,6-isomers, molar ratio 65/35), with oligomeric butylene adipate glycol, BAG (molar mass 2000) in 70% solution in ethyl acetate (molar proportion of reagents 1.01/1.00, catalyst: tin dibutyl laurate, 0.2 wt %).

The poly(styrene-*b*-acrylic acid) copolymer (S-*b*-AA, acid form) was obtained by emulsion block-copolymerization carried out in a glass reactor under nitrogen (15 h at 60°C). Styrene and acrylic acid were distilled under vacuum at temperatures 20–25°C and 42–45°C, respectively, and stored at −15°C prior to use. The distillations were performed no more than 24 h prior to polymerization. First, the acrylic acid (12 mL), ammonium persulfate initiator (1 g), and sodium lauryl sulfate stabilizer (3 g) were dissolved and mixed with deionized water (100 mL) for 30 min. Then, styrene was added gradually (by drops) for 4 h at continual mixing of the emulsion up to the end of reaction. The reaction product was coagulated by hydrochloric acid solution (0.1*N*), washed by ethanol (50 mL) and by deionized water until pH = 7.0, filtered, and vacuum-dried. Finally, the polymer obtained was dissolved in dioxane, precipitated by water, filtered, and vacuum-dried. The molar ratio of S/AA in S-*b*-AA was approximately 90/10 (estimated from carboxyl group content by base titration).

The chemical structure of both components is given in Scheme 1.

Films, 0.2–0.5 mm thick, of thermoplastic apparent IPNs of several compositions were prepared by casting from 20% solution in dioxane onto Teflon plates and subsequent evacuation to constant weight.

Methods

The molecular mass distribution (MMD) of the individual CPU and S-*b*-AA components was estimated by size exclusion chromatography (SEC) using the Du Pont LC System 8800 with ultraviolet detector with wavelength 280 nm and bimodal exclusion columns AZorbax@. Chloroform containing 5% of methanol was used as solvent. Sample weight was 0.01–0.02 g. The calibration of columns was carried out with polystyrene standard of molar mass 30,000 and polydispersity index $M_w/M_n = 1$.

Differential scanning calorimetry (DSC) measurements were carried out using a PerkinElmer Pyris 1 DSC under nitrogen flux in the temperature range from −60 to 175°C with a programmed heating rate of 20 K/min. The sample weight was 10–15 mg. All DSC curves were baseline subtracted and normalized to 1 mg of sample. The second heating scan was taken for

CPU - crystallizable polyurethane:

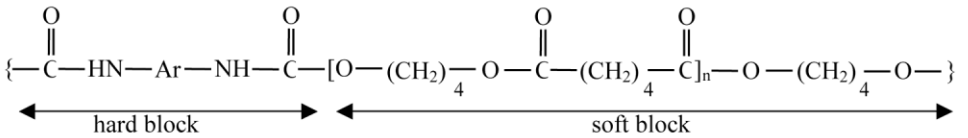

where Ar:

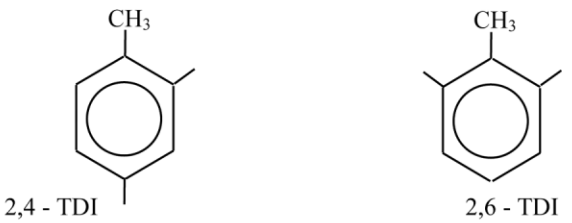

S-*b*-AA - poly(styrene-*b*-acrylic acid), acid form:

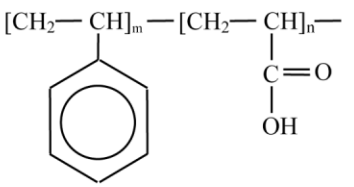

Scheme 1 Chemical structure of the neat CPU and S-*b*-AA components.

data analysis. The temperature dependence of the heat capacity C_p was determined and the midpoint of the endothermic jump of the function $C_p = f(T)$ was taken as the glass transition temperature (T_g). For melting events, the melting temperature (T_m) was taken as the temperature corresponding to the maximum in fusion endotherm and the heat of fusion (ΔH) was calculated from the area under the endothermic peak.[16]

The density (average value over five measurements) of the samples was determined using Archimedes's method, at room temperature.

Thermogravimetric analysis (TGA) was performed using the Q-1500D Derivatograph system developed by F. Paulik, J. Paulik and L. Erdey (Magyar Optikai Müvek, Budapest, Hungary). TGA traces were registered in the temperature range from 25 to 660°C at a heating rate of 10 K/min in air by evacuating the volatile products. The sample weight was 50 mg.

Dynamic mechanical analysis (DMA) measurements were obtained on a viscoelastometer (in tensile test mode), with temperature scans from −80 to 140°C at a frequency of 100 Hz. The heating rate was 2 K/min, and the dimensions of the sample 0.5 × 6.0 × 0.02 mm^3. The storage modulus (E') and the loss modulus (E'') were calculated from measurements of the complex modulus (E) and plotted versus temperature.

For dielectric relaxation spectroscopy (DRS) measurements,[17] the complex dielectric permittivity, $\varepsilon^* = \varepsilon' - i\varepsilon''$, was determined as a function of frequency (10^{-2} to 10^6 Hz) at constant temperature (controlled to better than ± 0.1°C). A Schlumberger Frequency Response Analyzer (FRA SI 1260) supplemented by a buffer amplifier of variable gain (Chelsea Dielectric Interface) in combination with the Novocontrol Quatro System were used. The samples were circular films of typically 20 mm diameter and 0.2–0.5 mm thickness.

The thermally stimulated depolarization currents (TSDC) method consists of measuring the thermally activated release of stored dielectric polarization.[18] A homemade experimental apparatus was used for measurements, details being given in previous publications.[12–14] The TSDC method corresponds to measuring dielectric losses as a function of temperature at a fixed low frequency (equivalent frequency) in the range 10^{-2} to 10^{-4} Hz.

RESULTS AND DISCUSSION

Molar mass distribution

The molecular mass distribution (MMD) has been investigated for the neat CPU and S-*b*-AA components,

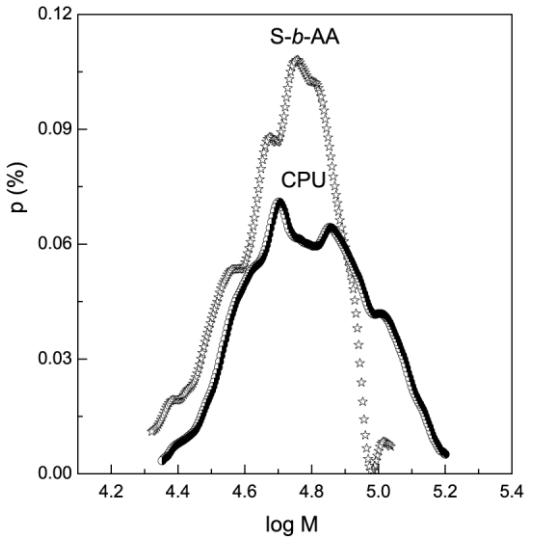

Figure 1 Molecular mass distribution (MMD) chromatograms for individual CPU and S-*b*-AA.

aiming to determine the characteristics of the distribution and to check the purity of the polymers, the corresponding curves being shown in Figure 1. The MMD characteristics of the neat polymers are as follows: CPU—M_w ~67,000, M_n ~56,900, M_z ~78,400, and M_w/M_n ~1.18; S-*b*-AA—M_w ~53,800, M_n ~48,800, M_z ~58,400, and M_w/M_n ~1.10, where M_w, M_n, and M_z are the weight–average, the number–average, and the *Z*-average molar mass, respectively. In general, one can conclude that both CPU and S-*b*-AA are characterized by quite high-molecular masses and low-polydispersity indices (M_w/M_n). However, CPU is characterized by higher M_w, M_n, and M_z values, as compared to S-*b*-AA. Furthermore, no low-molecular mass fractions are present in neither the CPU nor the S-*b*-AA components. Consequently, no postcuring reactions are expected to occur during heating the samples in the various experimental tests.

Morphology

Figure 2 shows DRS results at room temperature (25°C): real part of dielectric permittivity ε' (a), imaginary part (dielectric loss) ε'' (b), and ac conductivity σ_{ac} (c) in a broad frequency range for the pure CPU and S-*b*-AA components and several t-AIPNs indicated on the plot. σ_{ac} (actually, real part σ'_{ac} of the complex conductivity) was calculated from the measured loss values by[17]

$$\sigma_{ac}(f) = 2\pi f \varepsilon_0 \varepsilon''(f) \quad (1)$$

where f the frequency of the applied electric field and ε_0 the permittivity of free space. The temperature of measurements is above the glass transition temperature T_g of the amorphous phase of CPU and below that of the copolymer, as will be shown by DSC later. For that reason and, although melting of the crystalline phase of CPU occurs at a higher temperature, in the range 40–50°C (see below), CPU is characterized by much higher mobility than the copolymer. The high values of ε' at frequencies lower than about 10 Hz in CPU and in some of the t-AIPNs, which increase with decreasing frequency, do not reflect bulk properties, but are rather related with space charge polarization due to dc conductivity, as indicated by the frequency dependence of ε'' and of σ_{ac}.[19]

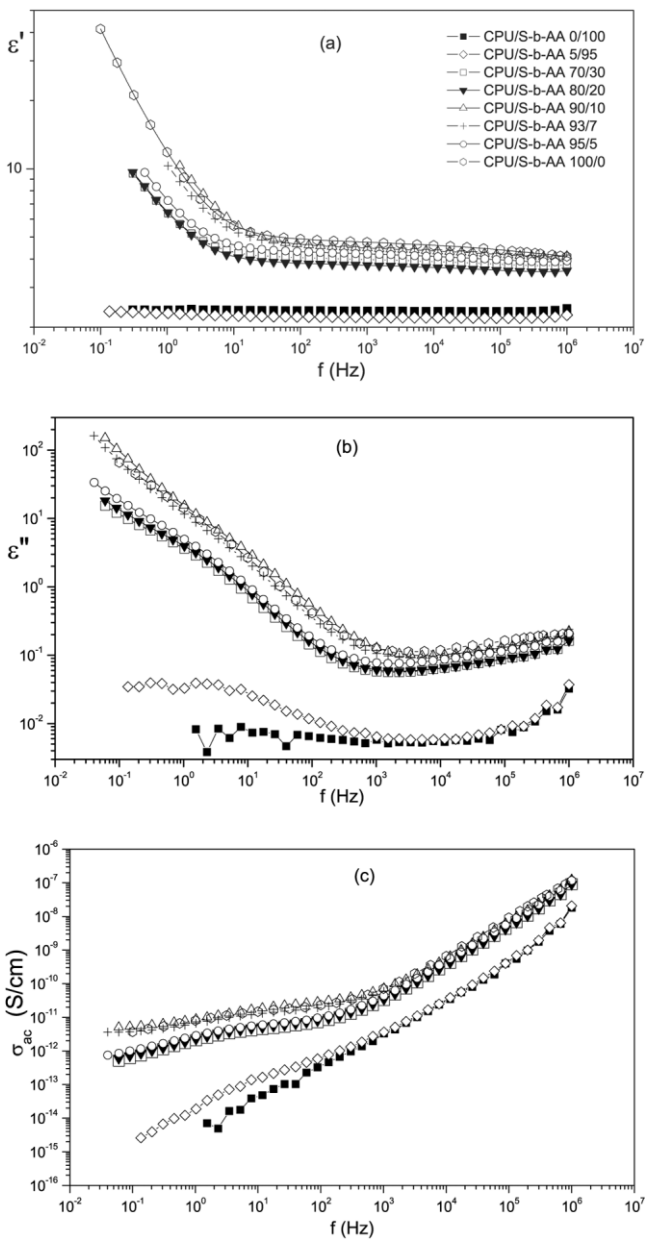

Figure 2 Real, ε'(a) and imaginary part, ε'' (b) of dielectric permittivity and ac conductivity, σ_{ac} (c) of the samples indicated on the plot against frequency f at 25°C.

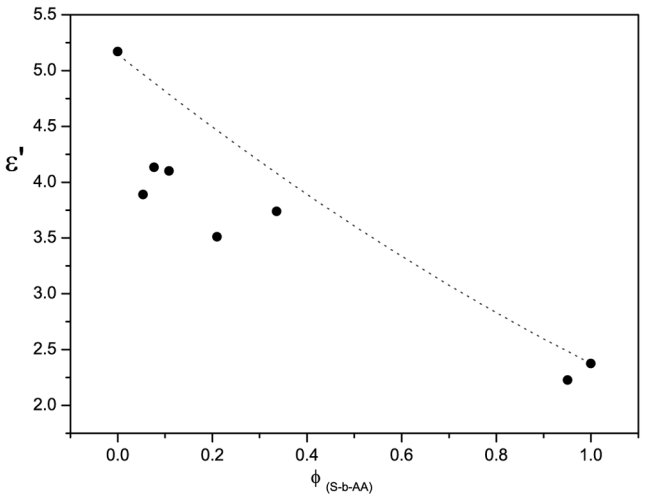

Figure 3 Real part of dielectric permittivity ε' against copolymer content of the t-IPNs at $f = 0.7$ MHz. The line is the prediction of eq. (2).

The significantly different level of molecular mobility of the two IPN components, indicated in Figure 2, in particular that of macroscopic charge carrier motion giving rise to conductivity effects, forms the basis for morphological characterization of the t-AIPNs by DRS in terms of phase continuity. The samples can be classified into two groups on the basis of the results shown in Figure 2: the pure copolymer and sample CPU/S-*b*-AA 5/95 form the first group, whereas all the other samples belong to the second group. The samples of the first group are characterized by low values of ε' and the absence of conductivity effects. In the samples of the second group rather high values of ε' are measured and conductivity effects dominate at low frequencies.

ε' in Figure 2 at higher frequencies, where conductivity effects are absent, increases in general with decreasing copolymer content in the t-AIPNs. Figure 3 shows the dependence of ε' on S-*b*-AA content at a fixed high frequency, $f = 0.7$ MHz. The line in Figure 3 is the prediction of the symmetric Bruggeman equation,[20]

$$\frac{\varepsilon_m - \varepsilon_2}{\varepsilon_1 - \varepsilon_2}\left(\frac{\varepsilon_2}{\varepsilon_m}\right)^{1/3} = 1 - \phi_2 \qquad (2)$$

that is, calculated on the basis of mean field theories for noninteracting S-*b*-AA and CPU phases. In this equation ε_m, ε_1, and ε_2 are the dielectric permittivity of the composite, the host phase and the inclusion phase, respectively, and φ_2 is the volume fraction of the inclusion phase. We observe in Figures 2 and 3 deviations from a monotonous decrease of ε' with increasing copolymer content, in particular on addition of small amounts of either of the components, indicating interactions between the two components. Similar results were obtained also in previous work with the t-AIPNs based on the same CPU and a random S/AA copolymer and explained in terms of physical interactions of the COOH-groups of AA in S/AA with the ester groups of the flexible CPU blocks, which promote microphase separation in both the CPU and the copolymer components.[12–14] The same explanation holds also for the results presented in Figures 2 and 3. Such interactions may also lead to a decrease of the degree of crystallinity of CPU in the t-AIPNs, resulting in increase of ε' (as will be shown by DRS measurements at higher temperatures later in this section). In fact, DSC measurements to be reported later in this section indicated a slight decrease of the degree of crystallinity of CPU in the t-AIPNs, in agreement with the results of DSC and mechanical spectroscopy on the salt (potassium) form of samples similar to those investigated here.[21] The decrease of the degree of crystallinity of CPU in the t-AIPNs could contribute to the increasing of ε' of the samples with 93 and 90% CPU above that of the sample with 95% CPU and of the sample with 70% CPU above that of the sample with 80% CPU in Figures 2 and 3.

A classification of t-AIPNs into two groups on the basis of DRS measurements, similar to that in the present work, was observed before also for the t-AIPNs based on the random S/AA copolymer.[12–14] In that case, more copolymer-rich samples could be prepared and investigated and the results by DRS were in agreement with those obtained by SAXS.[12] Obviously, morphological characterization in terms of phase continuity on the basis of DRS measurements is more critical in the case of samples with composition around 50:50. In the previous work on the t-AIPNs based on the random S/AA copolymer, CPU phase continuity was observed for the sample with 50 wt % CPU.[12]

We turn now our attention to the results obtained by DSC. The DSC curves of pure CPU and S-*b*-AA, as well as of CPU/S-*b*-AA t-AIPNs with various compositions, are presented in Figures 4 and 5, whereas the corresponding thermal characteristics are summarized in Table I. The DSC thermogram of pure CPU is characterized by the presence of both the small jump at the glass transition temperature $T_g = -44$°C of the amorphous quasiphase of the semicrystalline CPU (Figs. 4 and 5) and the broad melting endotherm (heat of fusion $\Delta H_m \approx 51$ J g^{-1}) with two sharp maxima at $T = 37.9$°C and at $T = 47.6$°C due to melting of the BAG microcrystals of CPU.[10] The first maximum at $T = 37.9$°C is connected with the process of melting of less perfect crystallites followed by recrystallization in the temperature range up to $T \approx 41.7$°C and further melting at $T_m = 47.6$°C. The degree of crystallinity X_c of the neat CPU calculated from WAXS data in our previous paper[12] was equal to $X_c \approx 49\%$. Note that

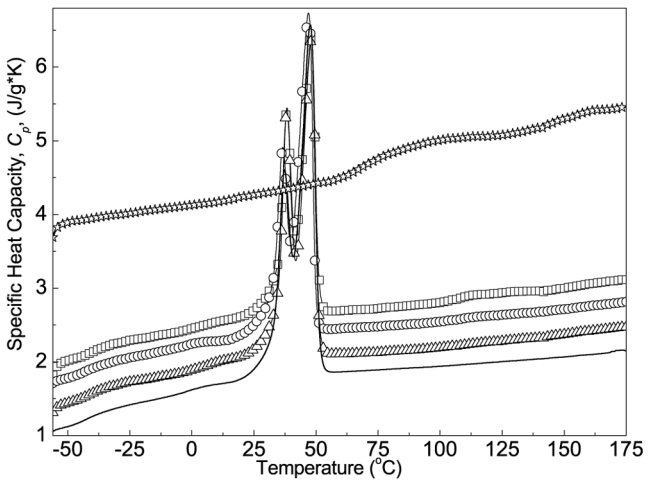

Figure 4 Typical DSC traces for the individual CPU (solid line) and S-*b*-AA (■) components and for the CPU/S-*b*-AA t-AIPNs of composition (wt %): 95/5 (△); 90/10 (○); and 80/20 (□). The curves have been shifted vertically for clarity.

only one sharp melting maximum was observed for CPU in the first heating scan, not shown here (T_m = 50.2°C, $\Delta H_m \approx 73$ J g^{-1}, $T_g = -39.2$°C).

In contrast to CPU, two sudden jumps at the glass transition temperatures T_{g1} ~70°C and T_{g2} ~144°C are observed on heating the neat S-*b*-AA component (Fig. 4 and Table II). Therefore, S-*b*-AA can be regarded as a wholly amorphous system, which is characterized by its own microphase-separated structure. We consider that this can be caused by the true microphase separation between the styrene (T_{g1}) and the acrylic acid (T_{g2}) blocks in S-*b*-AA, due to the formation of hydrogen bonds between COOH-groups of AA in S-*b*-AA,[22,23] and/or by the presence of absorbed (bound) water, that acts as natural plasticizer for S-*b*-AA forming intermolecular hydrogen bonds with polar (carboxylic) groups of S-*b*-AA.[24] Indeed, it was found that the S-*b*-AA sample involves approximately 3.9 wt % of bound water. However, according to TGA data to be reported later in this section, only about 1.2 wt % of loss mass is observed on heating the neat S-*b*-AA component up to 180°C. Recall please that the second heating scan was taken for DSC data analysis. Thus, we consider that the sample has not been completely dried during the first heating scan of the sample. This conclusion is in agreement with DSC data shown in Figure 6 for styrene–acrylic acid random copolymer (S-*co*-AA) with high acrylic acid content, S/AA = 55/45 wt %, and about 6.5 wt % of bound water: at least three different T_g values are observed during the first heating scan, however only a single T_g after heating the sample at T = 250°C for 15 min.

The DSC thermograms in Figure 4 show the presence of large melting endotherms of the BAG microcrystals of the CPU component in all the t-AIPNs studied. Close inspection of the thermal characteristics of the crystalline phase of the CPU component T_m, ΔT_m, and ΔH_m shown in Table I, forces us to conclude that incorporation of S-*b*-AA into the CPU matrix does not change significantly the characteristics of the endothermic melting process. However, we observe in Table I that the experimental ΔH_m values, calculated per unit mass of the blends, decrease on addition of small amount of S-*b*-AA (already 5 wt %), as compared to the values calculated on the basis of additivity. This fact means that the CPU component in the blends has a lower degree of crystallinity, as compared to pure CPU, in agreement with the results of DSC and DMA on the salt (potassium) form of samples similar to those investigated here.[21] At the same time, T_g of CPU increases slightly on addition of S-*b*-AA in the t-AIPNs, as compared to pure CPU, whereas T_g of S-*b*-AA decreases (Table I). Thus, some convergence of the T_g values of the CPU and S-*b*-AA components is observed in their blends on increase of the S-*b*-AA content from 5 to 20 wt %, providing evidence of some improving compatibility of the components, at least in the amorphous phase. Both effects, the decrease of the degree of crystallinity of the CPU component and the improvement of the compatibility of the two components in the t-AIPNs, are attributed to the formation of new intermolecular network of hydrogen bonds between the functional groups of the two components, i.e., urethane and ester groups of the flexible blocks of CPU and COOH-groups of AA in S-*b*-AA. This intermolecular hydrogen bonding promotes the formation of a mixed amorphous phase, characterized by a higher T_g than that of pure CPU, and provides also a hindrance to crystallizability of CPU in the t-AIPNs.

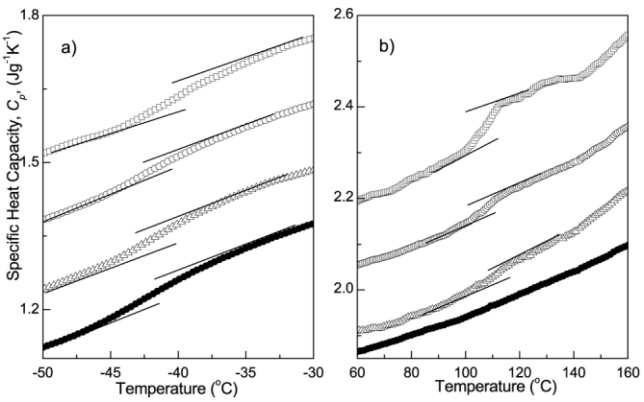

Figure 5 DSC thermograms in the glass transition temperature regions (marked by solid lines) of CPU (a) and S-*b*-AA (b) obtained with the individual CPU (●) and the CPU/S-*b*-AA t-AIPNs of composition (wt %): 95/5 (△); 90/10 (○); 80/20 (□). The curves have been shifted vertically for clarity.

TABLE I
T_m and T_g Values (DSC Data) for the Individual Polymers and for the CPU/S-*b*-AA Compositions Studied

Composition (wt %)	T_m (°C)	$T_{m\ onset}/T_{m\ end}$ (°C)	ΔT_m (°C)	ΔH_m[a] (J/g)	$\Delta H_{m\ add}$[b] (J/g)	T_g (°C) for phases rich in: CPU	S-*b*-AA
CPU	47.6	17/56	39	50.5	50.5	−44	—
S-*b*-AA	—	—	—	0	0	—	69; 144
CPU:S-*b*-AA							
95:5	47.8	17/55	38	44.3	48.0	−42	111
90:10	47.1	15/55	40	42.3	45.4	−42	108
80:20	47.8	17/55	38	36.4	40.4	−40	107

[a] ΔH_m is the melting heat of the BAG microcrystals of the CPU component. The ΔH_m values were calculated per unit mass of the blends.
[b] $\Delta H_{m\ add}$ values were calculated by assuming for CPU its original value of ΔH_m and additivity of the contributions of the two components.

Additional information on phase morphology and thermal transitions was provided by thermomechanical analysis. Figure 7 depicts the temperature dependence of loss modulus E'' for the individual CPU and S-*b*-AA components, as well as for selected CPU/S-*b*-AA t-AIPNs, the corresponding DMA characteristics being summarized in Table II. The mechanical spectra of pure CPU are typical for biphasic semicrystalline polymers.[25,26] Two transitions are observed: the α transition associated with the glass transition of the amorphous phase as a main peak at −22°C; and the α_c transition associated with motions in the crystalline portion of the polymer as a weak shoulder in the region from −5 to + 20°C. (Please note that these two transitions in semicrystalline polymers labeled β and α, respectively,[26]). In the region of temperatures around 50°C melting of BAG microcrystallites of the CPU component begins, in agreement with the DSC results reported earlier. The mechanical spectra of the individual S-*b*-AA component show the dynamic glass transition (T_g) at 86°C (Table II) and a shoulder at about 111°C (Fig. 7), which is indicative of limited heterogeneity of the S-*b*-AA component, as discussed earlier. Please note, also for the following discussion, that glass transition temperatures by DMA are shifted to higher temperatures, with respect to DSC, because of the higher frequency of measurements of the former (100 Hz against an equivalent frequency in the range of mHz for DSC[14]).

We observe in Table II that T_g values of the CPU component in the CPU/S-*b*-AA t-AIPNs with S-*b*-AA content 5–30 wt % are close to T_g of the individual CPU, providing evidence of a two-phase morphology of the compositions studied. Note that it was impossible to estimate T_g for the S-*b*-AA component in the CPU-rich compositions, due to softening and breaking of the samples during melting of the CPU matrix. Nevertheless, slightly increasing T_g values of the CPU component in the t-AIPNs, as compared to the indi-

TABLE II
DMTA Data for the Individual Polymers and the Blends Studied

Composition (wt %)	T_g (°C)/E''[a] (MPa) for phases rich in: CPU T_{g1}/E''_1	S-*b*-AA T_{g2}/E''_2
S-*b*-AA	—	86/65; 112/21
CPU	−22/60	—
CPU:S-*b*-AA		
95:5	−22/55	ND
90:10	−22/53	ND
80:20	−21/48	ND
70:30	−20/36	ND
20:80	−12/23	76/57
10:90	−10/20	80/63

ND: It was impossible to determine due to softening and breaking of the samples.
[a] E''_i value taken at T_{gi}.

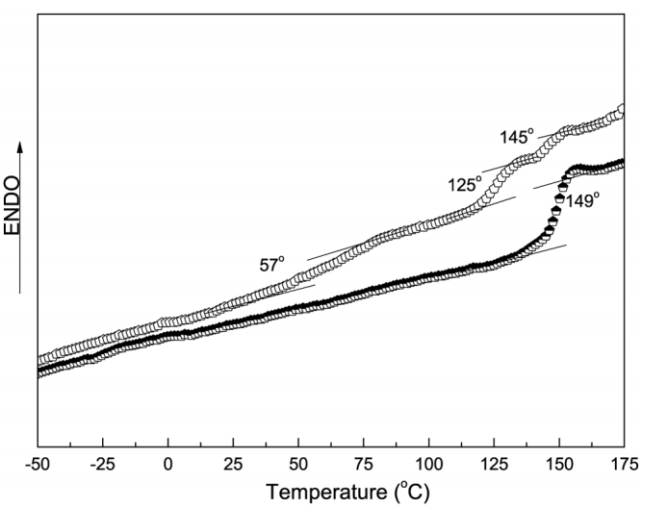

Figure 6 DSC traces for neat S-*co*-AA (S/AA = 55/45 wt %) (□) and for the same sample after heating at T = 250°C for 15 min (■).

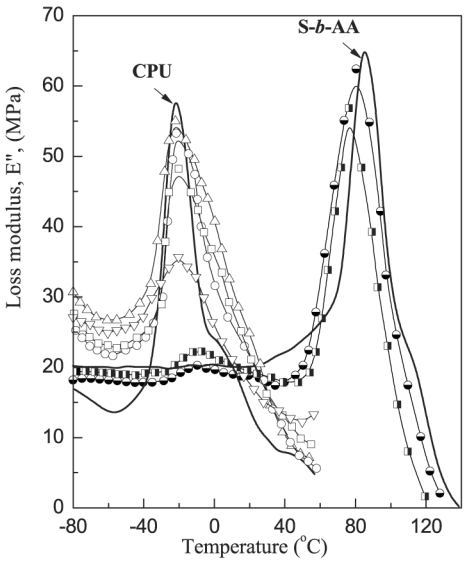

Figure 7 Temperature dependence of mechanical loss modulus (E'') for the individual CPU and S-*b*-AA components and for CPU/S-*b*-AA t-AIPNs of composition (wt %): 95/5 (△); 90/10 (○); 80/20 (□); 70/30 (▽) 20/80 (■); and 10/90 (●).

vidual CPU, and some expansion of the glass transition region (Fig. 7), observed at increasing of the S-*b*-AA content in the blends, provide evidence of improving of components compatibility, obviously due to formation of some interfacial layer where both of the components are interpenetrated. Therefore, it can be concluded that some hampering of the segmental mobility of the CPU chains has occurred in the amorphous phase of the blends studied.

Significant hampering of the segmental mobility of the CPU chains is observed in Figure 7 and Table II for the blends with high content of the S-*b*-AA component (80 and 90 wt %), where the S-*b*-AA component forms the matrix. It can be seen that T_g of the CPU component has increased by 12 and 10°C and, simultaneously, T_g of the S-*b*-AA component has decreased by 5 and 9°C for the blends with S-*b*-AA content of 90 and 80 wt %, respectively. All these facts provide evidence for both the changing of microphase structure of the t-AIPNs studied and the improving compatibility of the components in the t-AIPNs.

Summarizing, the DRS, DSC, and DMA data presented in this section show that the CPU/S-*b*-AA t-AIPNs studied can be considered as multiphase systems having at least two amorphous and one crystalline phases, as well as regions of mixed compositions. Their properties, to be studied also in a next section, are determined by the heterogeneity of the individual components, as well as by the heterogeneity caused by the thermodynamic incompatibility of these components. The degree of incompatibility is determined, to a large extent, by the intermolecular hydrogen bonding between the functional groups of the CPU and the S-*b*-AA components.

Molecular mobility

Figure 8 shows results of TSDC measurements obtained with the t-AIPN with 5% copolymer and with the pure copolymer at temperatures below room temperature. The TSDC thermograms correspond to measuring dielectric loss against temperature at a fixed low frequency in the range 10^{-2} to 10^{-4} Hz and provide a quick characterization of the overall dielectric behavior of the material under investigation.[18] The thermogram recorded with sample CPU/S-*b*-AA 95/5 is representative for the CPU rich samples and shows similarities with thermograms recorded in previous work with t-AIPNs based on CPU and a random S/AA copolymer.[12–14] Four TSDC peaks are observed in this thermogram, all of them attributed to the CPU component, namely, in the order of increasing temperature, to the local, secondary γ and β relaxations, the cooperative, segmental α relaxation, associated with the glass transition of the amorphous SS phase of CPU, and the interfacial Maxwell–Wagner–Sillars (MWS) relaxation, associated with accumulation and subsequent release of charges at the interfaces between HS domains and SS microphase.[12–14] The secondary γ and β relaxations in PUs, observed also by mechanical spectroscopy, have been attributed to crankshaft motions of methylene, $(CH_2)_n$, sequences and to associations of absorbed water molecules with the polar carbonyl groups, respectively.[12]

The TSDC thermogram recorded on the neat S-*b*-AA in Figure 8 shows at low temperatures only a weak peak at about −130°C, in agreement with TSDC measurements on the random S/AA copolymer of the previous work. This peak has been assigned to the β

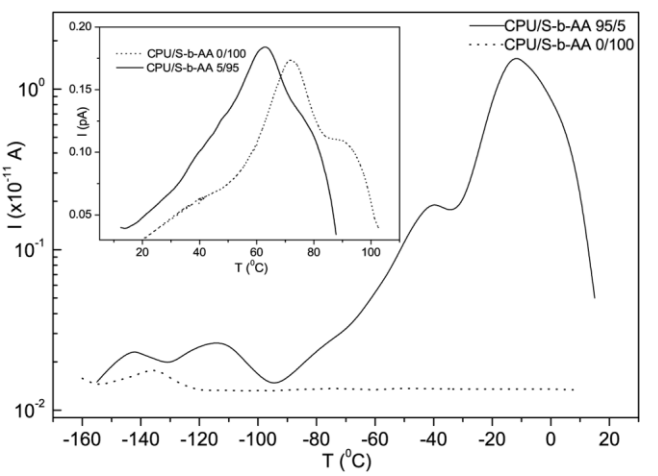

Figure 8 TSDC thermograms recorded with the samples indicated on the plot.

relaxation of the acrylic units, i.e., to the rotation of the —COOH side group about the C—C bond, which links it to the main chain.[12] In support of this interpretation, the TSDC β peak of the block copolymer is much weaker than the corresponding peak of the random copolymer of the previous work,[12] reflecting the lower fraction of AA in the block (10%) than in the random copolymer (28%).

The inset to Figure 8 shows TSDC thermograms at high temperatures to follow the α relaxation associated with the glass transition of the copolymer. The thermogram for the neat copolymer exhibits a main peak at about 70°C and a second weaker one at about 90°C. Please note the similarity to the DMA plot in Figure 7, the main difference being the shift of the mechanical loss peaks to higher temperatures, due to the higher frequency of DMA measurements. In agreement with the results of DSC and DMA measurements in the previous section, the main peak is attributed to the α relaxation associated with the glass transition of the copolymer. Interestingly, DSC and DMA measurements on the salt (potassium) form of the same copolymer give T_g values in the same temperature region, 70–80°C.[21] The second peak at about 90°C is attributed to a second glass transition in the copolymer, reflecting some degree of microphase separation, in agreement with the block character of the copolymer and the results of DSC and DMA measurements on the t-AIPNs reported in the previous section.

Changes in the characteristics of the TSDC peaks with composition reflect changes in the morphology of the samples under investigation and may be discussed in terms of interaction between the IPN components. The following discussion is based mainly on the temperature position of the peaks, corresponding to the time scale of the response, and to a lesser extent on the magnitude (dielectric strength) and the shape of the peak. This discussion will not be limited to the α peaks, associated with glass transitions investigated by DSC and DMA in the previous section, but will include the interfacial MWS peak and the secondary peaks. The inclusion of the MWS peak is obvious, as this peak reflects morphological properties.[13] On the other hand, dielectric measurements on nanostructured polymeric systems, including organic–inorganic nanocomposites, have indicated significant effects on the secondary relaxations of the polymeric components, often explained in terms of changes of free volume and/or specific interactions between the individual components.[27]

Starting with the relaxations of the copolymer, both TSDC α peaks associated with glass transitions in the copolymer, the main at about 70°C and a weaker one at about 90°C, are shifted by about 10°C to lower temperatures on addition of 5% CPU (Fig. 8). A similar shift for the main peak has been observed by DMA in the t-AIPNs with 10 and 20% CPU (Fig. 7 and Table II).

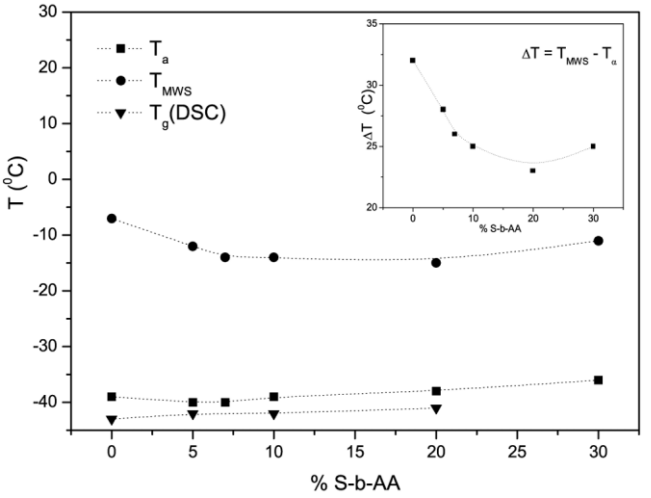

Figure 9 TSDC peak temperatures T_α and T_{MWS}, glass transition temperature T_g and $\Delta T = T_{MWS} - T_\alpha$ (inset) against copolymer content in the CPU-rich t-AIPNs.

This result indicates partial miscibility of the two components, explained in terms of physical interactions, as discussed in the previous section. The α relaxation of the copolymer could not be followed in the CPU-rich samples neither by TSDC nor by DRS (in contrast to the associated glass transition, which could be followed by DSC), as it is masked by conductivity effects, arising from high conductivity of CPU at higher temperatures (compare Fig. 2). The same holds also for the DMA results reported in the previous section (Fig. 7 and Table II), however, for a different reason, namely softening and breaking of the samples during melting of the CPU matrix. The weak β relaxation of the copolymer is absent in the thermogram of the t-AIPN with the highest copolymer fraction, sample CPU/S-*b*-AA 5/95 (not shown in Fig. 8), which could not be expected on the basis of additivity and the high sensitivity of TSDC. This result indicates suppression of the β relaxation of the copolymer in the t-AIPNs and can be understood in terms of involvement of the —COOH side groups, responsible for the relaxation, in physical interactions (hydrogen bonding) with the ester groups of CPU. Interestingly, suppression of the β relaxation of the copolymer was observed also in the salt form of the IPNs under investigation here by DMA.[21]

Figure 9 shows results for the dependence of the TSDC peak temperatures of the α relaxation of the CPU component, T_α, and of the MWS relaxation, T_{MWS}, on the copolymer content in the CPU-rich compositions. T_α increases slightly in the t-AIPNs with increasing amount of the copolymer, indicating that the α relaxation of CPU becomes slightly slower in the IPNs, whereas T_{MWS} decreases on addition of small amount of the copolymer, with respect to pure CPU, and then becomes stable. Results for the maximum

depolarization current for each peak, not shown here, indicate that the magnitude (relaxation strength) of the α relaxation does not practically change with composition, in contrast to that of the interfacial MWS relaxation, which increases in the compositions with 5 and 10% copolymer with respect to pure CPU. A first implication from these results is that changes in the characteristics of the MWS relaxation are more significant on addition of a small amount of the copolymer. Included in the figure are results for T_g determined by DSC, indicating very good agreement with T_α and providing additional evidence that T_α is a good measure of T_g.[14] DSC measurements on the salt form of the t-AIPNs under investigation here indicated, in agreement with the results reported here, that the α relaxation of CPU becomes slightly slower in the IPNs; however, these results were not confirmed by DMA.[21] The composition dependence of the characteristics of the α and of the MWS relaxation of the CPU component can be discussed in terms of modification of both the DMS[28] and of crystallinity of CPU in the t-AIPNs. Inherent to this discussion is the assumption (simplification) that the relaxations of the CPU component are not affected by the presence of the copolymer component in the t-AIPNs. In previous work on t-AIPNs based on a random S/AA copolymer evidence was provided for improved microphase separation (increase of DMS) of both components on mixing and explained in terms of physical interactions between the COOH-groups of AA in S/AA and the ester groups of the flexible CPU blocks.[12–14] This result is not confirmed here; on the contrary, $\Delta T = T_{MWS} - T_\alpha$ in the inset to Figure 9 decreases in the t-AIPNs, indicating decreased microphase separation in the CPU component in the mixtures.[28] This difference between the previous and the present t-AIPNs can be understood in terms of the lower fraction of AA in the block copolymers of the present t-AIPNs. The slight slowing down of the α relaxation of the CPU component in the t-AIPNs, observed by DSC, DMA, and TSDC in agreement with each other, is compatible with both a decreased microphase separation of the CPU component and a concomitant decrease of the degree of crystallinity of CPU, as indicated also by DRS results in the previous section. We will come back to this point later on the basis of DRS results for the α relaxation.

Results for the composition dependence of the TSDC peak temperatures of the secondary β and γ relaxations of the CPU component, T_β and T_γ, respectively, are shown in Figure 10. Similar to T_α and T_{MWS} in Figure 9, changes are more significant at small copolymer content, indicating interactions and partial miscibility of the IPN components. T_β decreases on addition of the copolymer, whereas T_γ first increases and then decreases. The magnitude of both relaxations, not shown here, also changes on mixing, that of

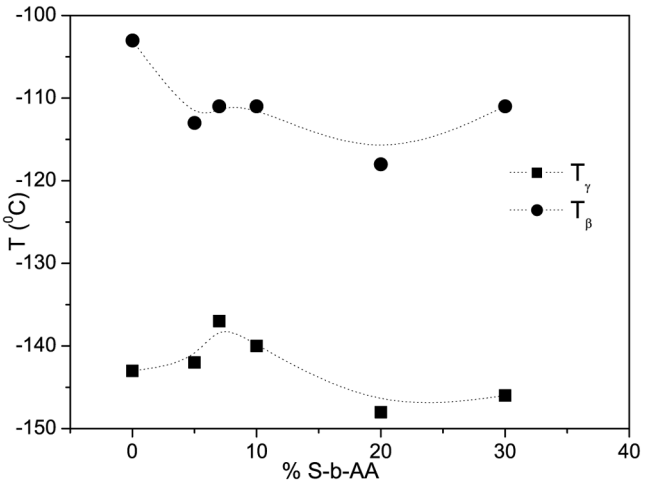

Figure 10 TSDC peak temperatures T_γ and T_β against copolymer content in the CPU-rich t-AIPNs.

the γ relaxation first increasing and then decreasing and that of the β relaxation increasing on addition of the copolymer. Increase of the magnitude of the mechanical γ relaxation was observed also in the salt form of the t-IPNs under investigation here and explained in terms of decrease of the degree of crystallinity of CPU on mixing of the two components.[21] One additional effect which has to be taken into account in understanding these results is that coming from the presence of moisture in the samples. The results reported earlier were obtained from measurements carried out on samples equilibrated in air. Dielectric measurements on PUs at various levels of relative humidity/water contents show, in agreement with DMA measurements,[21] that, on addition of water, the β relaxation becomes faster and the γ relaxation slower, whereas the magnitude of the former increases at the expense of that of the latter.[29] Measurements of water content show that, at the conditions of TSDC measurements, the water content of the samples in Figure 10 increases on addition of copolymer, being 0.12 and 0.37 g water per gram of dry sample in the t-AIPNs with 5 and 20 wt % copolymer, respectively. Thus, the results shown in Figure 10 arise partly from changes in water content and partly from morphological changes due to interactions between the two components.

The α relaxation of CPU in the t-AIPNs was studied in detail by DRS measurements. Frequency scans at several temperatures, not shown here, indicate that the relaxation becomes slightly slower on addition of the copolymer. Similar to other PUs,[28,29] the relaxation is, to a significant extent, masked by conductivity effects. Isochronal (constant frequency) plots can then reveal more details of the relaxation, in addition to providing a more direct comparison with DSC, DMA, and TSDC measurements. Figure 11 shows an isochronal plot of dielectric loss against temperature in

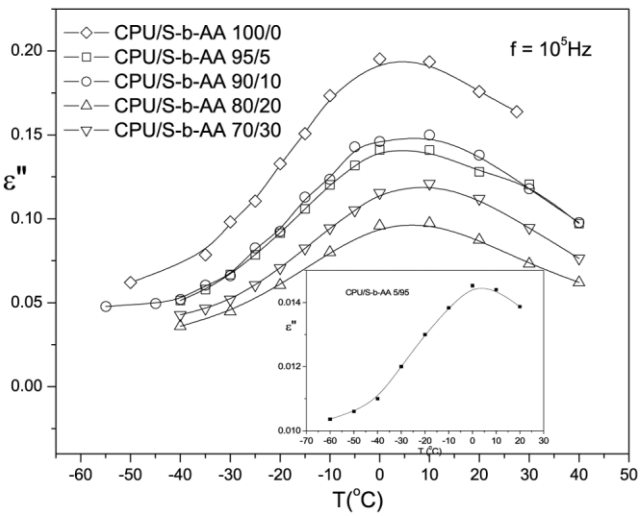

Figure 11 Isochronal (constant frequency, f = 100 kHz) plot of dielectric loss ε'' against temperature T in the region of the α relaxation of CPU of the samples indicated on the plot.

the region of the α relaxation of CPU in several t-AIPNs. A rather high frequency, f = 100 kHz, was chosen to eliminate effects of conductivity. For that reason the α relaxation is shifted to higher temperatures, as compared to DSC (Fig. 5) and TSDC (Figs. 8 and 9), which are characterized by equivalent frequencies in the range of mHz,[14] and to DMA measurements at 100 Hz (Fig. 7). We observe in Figure 11 that the α relaxation is slightly shifted to higher temperatures in the t-AIPNs, as compared to pure CPU, as confirmed also by the isothermal measurements not shown here, in agreement with the DSC and TSDC results. Please note that the DRS measurements were carried out on dry samples, thus eliminating any effects of moisture. The magnitude of the relaxation decreases in the t-AIPNs, in general, with increasing copolymer content. The decrease is nonmonotonous and, consistently, the same order of decrease is observed as in the $\varepsilon'(f)$ results at room temperature shown in Figure 2 (a). The decrease is larger than additivity would suggest. Please note, however, that a broadening of the peak is observed in the mixtures, which was not further evaluated quantitatively. The decrease of the degree of crystallinity of CPU on addition of the copolymer, indicated earlier, would result in an increase of the magnitude of the α relaxation. Thus, the results in Figure 11 suggest that this increase is overcompensated by the concomitant decrease due to constraints on the motion of the CPU chains imposed by the presence of and mixing with the copolymer and due to decrease of microphase separation of the CPU component, in agreement also with changes observed in the time scale of the α relaxation. The α loss peak was clearly observed also in the t-AIPN with the lowest amount of 5% CPU, as shown in the inset to Figure 11, this result providing strong support for a microphase-separated morphology of the t-AIPNs.

The time scale of the α relaxation of CPU was further evaluated. Figure 12 shows the Arrhenius plot (activation diagram, i.e., logarithm of frequency of maximum dielectric loss against reciprocal temperature) of the relaxation in pure CPU and in several CPU-rich t-AIPNs. The slowing down of the relaxation in the t-AIPNs, as compared to pure CPU is clearly observed. The results show also that the relaxation becomes slightly slower in the t-AIPNs with increasing copolymer content. The Vogel–Tammann–Fulcher (VTF) equation[30]

$$f_{\max} = f_0 \exp[-B/(T - T_0)] \tag{3}$$

which is characteristic for the cooperative glass transition was fitted to the DRS data obtained with CPU, and the values of the fitting parameters were determined to $f_0 = 2 \times 10^{13}$ Hz, B = 1029, and $T_0 = -60$°C. Because of the limited frequency range where data obtained with the mixtures could be evaluated, no attempts were made to fit eq. (3) to these data. The data suggest, however, a change of curvature, i.e., a change of fragility in the t-AIPNs. The concept of fragility, introduced by Angell,[31] has been much used in recent years to classify glass-forming materials with respect to kinetic and thermodynamic aspects of the glass transition. Several measures of fragility, i.e., the deviation from the Arrhenius behavior in the activation diagram, have been introduced. It has been suggested that fragility controls a number of properties, such as structural state dependence, decoupling phenomena, and nonexponentiality of relaxation. Fragility

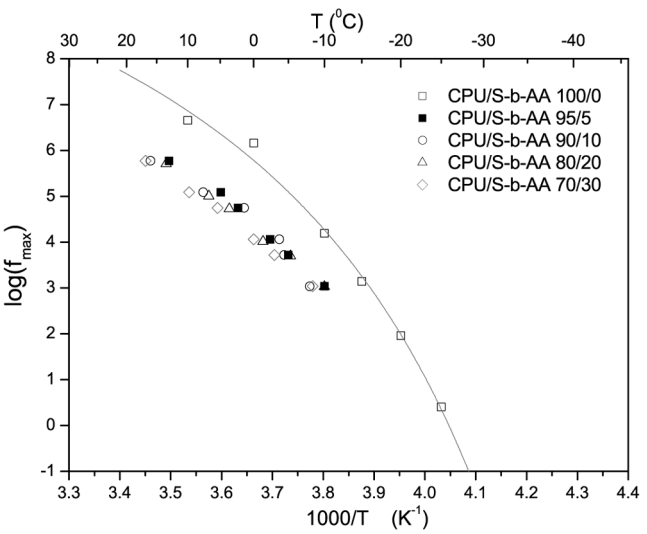

Figure 12 Arrhenius plot of the α relaxation of CPU in the samples indicated in the plot.

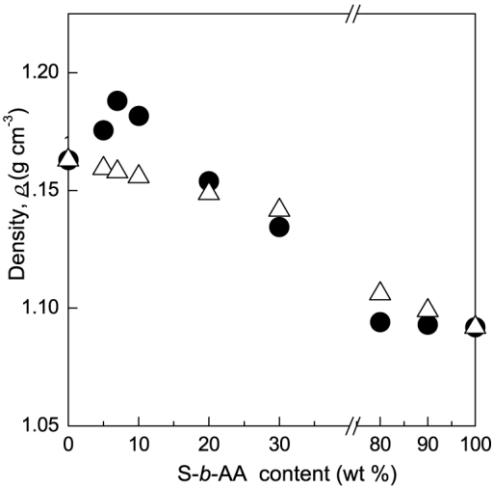

Figure 13 Concentration dependence of experimental (●) and additive (△) values of density of the CPU/S-*b*-AA t-AIPNs studied.

has been linked to the density of configurational and vibrational states, i.e., the density of minima in the potential energy hypersurface in configurational space, and the average barrier separating those minima.[31] The change of fragility in the t-AIPNS suggested by the data in Figure 12 is an interesting observation, which should be further followed in future work, as well as some differences, established above, in the pattern of the glass transition by dielectric techniques (DRS and TSDC) and by DMA on the one hand and by DSC on the other hand. It is interesting to note in this connection that DMA measurements on the salt form of the t-AIPNs under investigation here showed no change of T_g of CPU on addition of the copolymer, in contrast to calorimetric T_g, which was found to increase markedly, and that differences in the cooperative volumes probed by DSC or DMA were made responsible for that.[21]

Properties

The results of morphological and molecular dynamics characterization presented earlier indicate that the CPU/S-*b*-AA t-AIPNs studied can be considered as multiphase systems having at least two amorphous and one crystalline phases, as well as regions of mixed compositions. Thus, their properties, studied to some extent in the previous sections and also in the present section, can be expected to be determined by the heterogeneity of the individual components, as well as by the heterogeneity caused by the thermodynamic incompatibility of these components. The degree of incompatibility is determined, to a large extent, by the intermolecular hydrogen bonding between the functional groups of the CPU and the S-*b*-AA components.

Figure 13 shows results for the density of the t-AIPNs. The incorporation of 10–20 wt % of flexible CPU into the rigid S-*b*-AA matrix leads to decreasing of the density of the blends compared to the corresponding additive one. In general, density changes nonadditively with the change of composition. Also, it is known that the higher the density ρ, the higher the degree of crystallinity of the CPU component. Therefore, we suppose that lower density of the blends corresponds to lower degree of crystallinity of the CPU component, which, obviously, is caused by hampering of crystallization of the CPU component by the S-*b*-AA matrix of the blends. As a result, the amorphous part of the CPU component (which predominantly takes part in hydrogen bond formation) is increased, that leads to growth of the effective density of the network of intermolecular hydrogen bonds and results into improved compatibility of the components in the blends.

The thermal stability of the individual CPU and S-*b*-AA components, as well as of CPU/S-*b*-AA blends with S-*b*-AA content of 10, 20 and 30 wt % has been investigated by thermal gravimety analysis (TGA), the corresponding differential thermal gravimetry (DTG), and thermal gravimetry (TG) curves being shown in Figures 14(a,b) and 15(a,b), respectively. The TG and DTG parameters are summarized in Table III. The

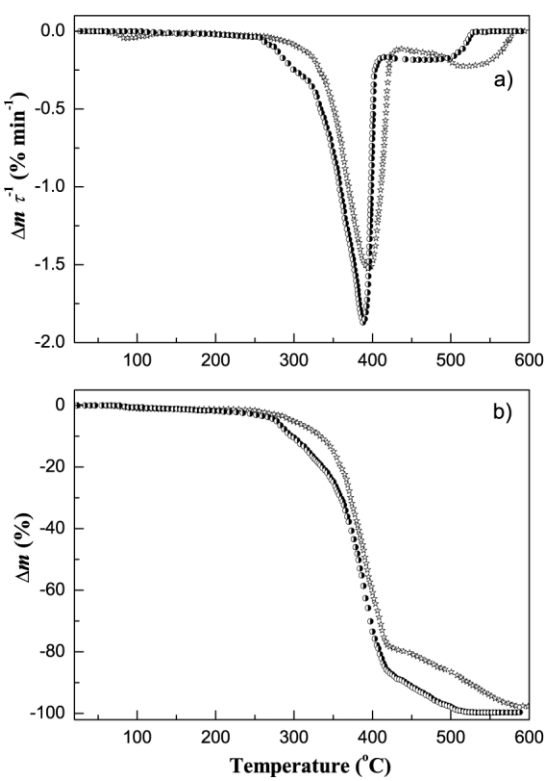

Figure 14 Thermogravimetric analysis curves for the individual CPU (○) and S-*b*-AA (□) components: (a) differential thermal gravimetry (DTG); (b) thermal gravimetry (TG).

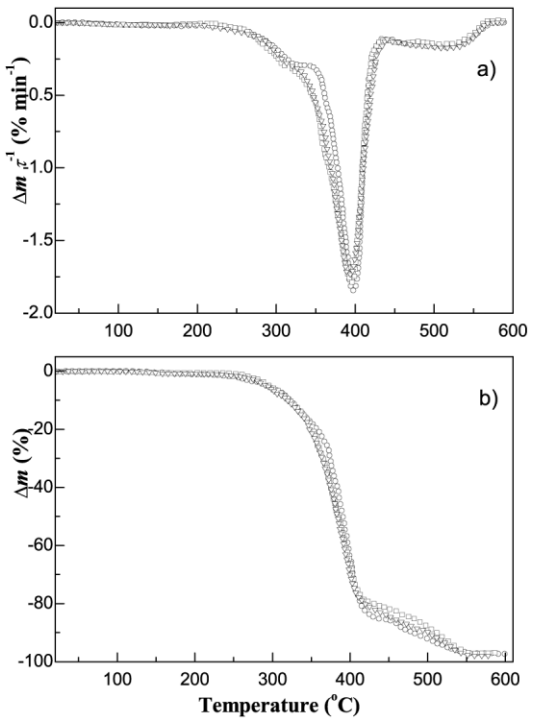

Figure 15 DTG (a) and TG (b) curves for the CPU/S-*b*-AA t-AIPNs of composition (wt %) 90/10 (○), 80/20 (□), and 70/30 (▽).

thermal decomposition of different polyurethanes has been investigated in detail in,[32,33] and the decomposition of polystyrenes as well as styrene copolymers in.[34–36] The TG/DTG curves of the individual CPU show that decomposition occurs in at least three steps, with decomposition temperatures ($T_{d\ \max}$) of 330, 388, and 475°C.[32,33] On the contrary, the TG/DTG curves of the individual S-*b*-AA show the existence of a two-step decomposition mechanism with decomposition temperatures $T_{d\ \max}$ of 394 and 530°C.[34–36] On the basis of the data presented in Table III one can conclude that the S-*b*-AA is characterized by higher thermostability compared to CPU, as it is characterized by higher values of onset temperature of decomposition and of $T_{d\ \max}$, as well as by lower values of weight loss.

The TGA data in Table III show that the CPU/S-*b*-AA blends containing 10, 20, and 30 wt % of S-*b*-AA are more stable than pure CPU. Indeed, all of the decomposition temperatures are higher for CPU in the blends compared to the neat CPU, whereas the corresponding values of weight loss *W* remain on the level of *W* values of the neat CPU or below that. Furthermore, one can see that all the blends studied are characterized by higher char residue values in comparison to the neat CPU.

All the facts mentioned earlier indicate that the conditions of decomposition of the CPU matrix were changed by the introduction of the S-*b*-AA component into the matrix, i.e., the presence of S-*b*-AA influenced both the values of $T_{d\ \max}$ and the corresponding *W* values of the CPU component. It is known[32–36] that if the mixing scale is poor, the decomposition of each polymer occurs independently of the presence of the other component. On the contrary, when the mixing of the two polymers reaches the molecular scale, a copyrolysis takes place with partial interactions. Due to overlapping of the degradation processes of the two components in Figures 14 and 15, it was not possible to identify the degradation process in the blends. However, the fact that the thermal stability of the CPU/S-*b*-AA blends is improved, as compared to the neat CPU, may be assumed to be due to intermolecular attraction between CPU and S-*b*-AA, so that more energy is required to overcome the intermolecular forces.

It is known[32] that the first low-temperature (200–300°C) decomposition of polyurethane is caused by dissociation of the urethane linkage of polyurethane that participates in hydrogen bonding, including intermolecular H-bonding with the COOH-groups of the S-*b*-AA component of the blends studied.[37] Since no any decomposition of the S-*b*-AA component is observed in that temperature range and the presence of S-*b*-AA increases the $T_{d1\ \text{onset}}$ value, we conclude that (1) $T_{d1\ \text{onset}}$ is the onset temperature of decompo-

TABLE III
TG/DTG Parameters for the Individual CPU and S-*b*-AA Components and for the CPU/S-*b*-AA t-AIPNs Studied

Composition (wt %)	Decomposition temperature, T_d (°C)						Weight loss, *W*, (wt %) at the temperature[a]:			Char residue values[a] (wt %)
	$T_{d1\ \text{onset}}$[a]	$T_{d1\ max}$[b]	$T_{d2\ \text{onset}}$	$T_{d2\ \max}$	$T_{d3\ \text{onset}}$	$T_{d3\ \max}$	$T_{d1\ \max}$	$T_{d2\ \max}$	$T_{d3\ \max}$	
CPU	263	330	330	388	430	475	20	62	95	0.3
S-*b*-AA	—	—	340	394	470	530	—	56	91	2.4
CPU:S-*b*-AA										
90:10	275	340	360	397	440	500	15	59	92	2.7
80:20	270	335	345	396	440	515	14	62	91	3.0
70:30	270	337	350	394	440	520	16	63	93	2.1

[a] Determined from the TG curve.
[b] Corresponding to the peak temperature of the DTG curve.

sition of the urethane linkage of the CPU component only; (2) the higher $T_{d1\ \mathrm{onset}}$ in the blends, as compared to the neat CPU, is caused by additional participation of urethane groups in hydrogen bonding with COOH-groups of the S-*b*-AA component of the blends studied, in agreement with DSC and DMA results reported earlier.

CONCLUSIONS

A variety of experimental techniques, to some extent complementary to each other, including SEC, DSC, TGA, DMA, DRS, TSDC, and density measurements were employed to investigate structure–property relationships of thermoplastic apparent interpenetrating polymer networks (t-AIPNs) of crystallizable polyurethane (CPU) and a styrene/acrylic acid block copolymer (S-*b*-AA, acid form) of several compositions, prepared by casting from a common solvent. The main results of this study can be summarized as follows.

1. With respect to morphology, the combined DRS, DSC, and DMA data show that the CPU/S-*b*-AA t-AIPNs studied can be considered as multiphase systems having at least two amorphous (a CPU and a copolymer) and one crystalline (CPU) phases, as well as regions of mixed compositions. Their morphological characteristics, including glass transitions of the amorphous phases and melting of the crystalline CPU phase, are determined by the heterogeneity of the individual components, as well as by the heterogeneity caused by the thermodynamic incompatibility of these components. The degree of incompatibility is determined, to a large extent, by the physical interactions (intermolecular hydrogen bonding) between the functional groups of the CPU and the S-*b*-AA components (ester groups and COOH-groups, respectively). To a large extent the phase-separated morphology of the two components is preserved in the t-AIPNs. However, T_g of CPU increases slightly on addition of S-*b*-AA in the t-AIPNs, as compared to pure CPU, whereas T_g of S-*b*-AA decreases. Thus, some convergence of the T_g values of the CPU and S-*b*-AA components is observed in their blends, providing evidence of some improving compatibility of the components, at least in the amorphous phase. At the same time, the degree of crystallinity of CPU decreases in the t-AIPNs. Both effects are attributed to the formation of new intermolecular network of hydrogen bonds between the functional groups of the two components, i.e., urethane and ester groups of the flexible blocks of CPU and COOH-groups of AA in the block copolymer.
2. From the methodological point of view, broadband DRS can be very effective for morphological characterization of the t-AIPNs (and similar complex systems). The significantly different level of molecular mobility of the two IPN components at room temperature, in particular that of macroscopic charge carrier motion giving rise to conductivity effects, forms the basis for that morphological characterization in terms of phase continuity.
3. Some differences were established in the pattern of the glass transition by DMA and dielectric DRS and TSDC techniques, employed to investigate the dynamic glass transition, on the one hand and by DSC on the other hand, which should be further followed in future work.
4. Molecular dynamics, in particular, that of CPU in the t-AIPNs, was studied in detail by dielectric DRS and TSDC techniques, additional information being provided also by DMA and DSC. Discussion was based mainly on the time scale of the various relaxations and to a lesser extent on the magnitude (dielectric strength) and the shape of the corresponding loss peaks. The discussion was not limited to the segmental α relaxation (dynamic glass transition), but was extended to include also the interfacial MWS relaxation and the local, secondary relaxations.
5. The segmental α relaxation of CPU was found to become slightly slower in the t-AIPNs, in consistency with the DSC and DMA data. At the same time the relaxation becomes broader, whereas its magnitude decreases, in general, with increasing copolymer content. The decrease is nonmonotonous and larger than additivity would suggest. The decrease of the degree of crystallinity of CPU on addition of the copolymer, indicated by DSC, would result in an increase of the magnitude of the α relaxation. Thus, the results suggest that this increase is overcompensated by the concomitant decrease due to constraints to the motion of the CPU chains imposed by the presence of and mixing with the copolymer and due to decrease of microphase separation of the CPU component, in agreement also with changes observed in the time scale of the α relaxation. The α loss peak was clearly observed also in the t-AIPN with the lowest amount of 5% CPU, this result providing strong support for a microphase-separated morphology of the t-AIPNs. In the Arrhenius diagram for the α relaxation of CPU a change of curvature was observed in the t-AIPNs, indicating a change of fragility, with respect to pure CPU. This is an interesting re-

sult, which should be further followed in future work.

6. Density was found to change, in general, nonadditevely with composition. Deviations from additivity are more significant on addition of small amounts of either of the components, due to interactions between their functional groups and formation of mixed microphases. One additional effect is that of the decrease of the density of the t-AIPNs on addition of 10–20 wt % of CPU with respect to additivity, in good correlation with the decrease of the degree of crystallinity of the CPU component in the t-AIPNs. The interactions between the functional groups of the two components and the resulting formation of mixed microphases affect also the thermal stability of the t-AIPNs. Thus, the thermal stability of the CPU component, i.e., that of the lower thermal stability, is improved in the t-AIPNs.

References

1. Koberstein, J. T.; Galambos, A. F.; Leung, L. M. Macromolecules 1992, 25, 6195.
2. Rizos, A. K.; Fytas, G.; Ma, R. J.; Wang, C. H.; Abetz, W.; Meyer, G. C. Macromolecules 1993, 26, 1869.
3. Hourston, D. J.; Schaefer, F.-U. Polymer 1996, 37, 3521.
4. Dadbin, S.; Burford, R. B.; Chaplin, R. P. Polymer 1996, 37, 785.
5. Pandit, S. B.; Nadkarni, V. M. Macromolecules 1994, 27, 4583.
6. Klempner, D.; Sperling, L. H.; Utracki, L. A., Eds. Interpenetrating Polymer Networks; Advances in Chemistry, Series 239; American Chemical Society: Washington, DC, 1994.
7. Klempner, D.; Frisch, K. C., Eds. Advances in Interpenetrating Polymer Networks, Vol. IV; Technomic: Lancaster, PA, 1994.
8. Sperling, L. H. Interpenetrating Polymer Networks and Related Materials; Plenum: New York, 1981.
9. Ali, S. A. M.; Hourston, D. J. In Advances in Interpenetrating Polymer Networks, Vol. IV; Klempner, D., Frisch, K. C., Eds.; Technomic: Lancaster, PA, 1994; p 17.
10. Sergeeva, L. M.; Grigoryeva, O. P.; Zimich, O. M.; Privalko, E. G.; Shtompel, V. I.; Privalko, V. P.; Pissis, P.; Kyritsis, A. J Adhes 1997, 64, 161.
11. Sergeeva, L. M.; Grigoryeva, O. P.; Brovko, A. A.; Zimich, O. N.; Nedashkovskaya, N.; Slinchenko, E.; Shtompel, V. I. J Prikladn Khim 1997, 70, 2038 (in Russian).
12. Kyritsis, A.; Pissis, P.; Grigorieva, O. P.; Sergeeva, L. M.; Brovko, A. A.; Zimich, O. N.; Privalko, E. G.; Shtompel, V. I.; Privalko, V. P. J Appl Polym Sci 1999, 73, 385.
13. Vatalis, A. S.; Delides, C. G.; Grigoryeva, O. P.; Sergeeva, L. M.; Brovko, A. A.; Zimich, O. N.; Shtompel, V. I.; Georgoussis, G.; Pissis, P. Polym Eng Sci 2000, 40, 2072.
14. Vatalis, A. S.; Delides, C. G.; Georgoussis, G.; Kyritsis, A.; Grigorieva, O. P.; Sergeeva, L. M.; Brovko, A. A.; Zimich, O. N.; Shtompel, V. I.; Neagu, E.; Pissis, P. Thermochim Acta 2001, 371, 87.
15. Tant, M. R.; Mauritz, K. A.; Wilkes, G. L., Eds. Ionomers; Chapman & Hall: London, 1997.
16. Bershtein, V. A.; Egorov, V. M. Differential Scanning Calorimetry of Polymers. Physics, Chemistry, Analysis, Technology; Ellis Horwood: New York, 1994.
17. Kremer, F.; Schoenhals, A., Eds. Broadband Dielectric Spectroscopy; Springer: Berlin, 2002.
18. Van Turnhout, J. In: Sessler, G. M., Ed.; Electrets: Topics in Applied Physics, Vol. 33; Springer: Berlin, 1980.
19. Kyritsis, A.; Pissis, P.; Grammatikakis, J. J Polym Sci Part B: Polym Phys 1995, 33, 1737.
20. Pelster, R. Phys Rev B: Solid State 1999, 14, 9214.
21. Bartolotta, A.; Carini, G.; D'Angelo, G.; Di Marco, G.; Farsaci, F.; Grigoryeva, O. P; Sergeeva, L. M; Slisenko, O.; Starostenko, O.; Tripodo, G. Philos Mag 2004, 84, 1591.
22. He, Y.; Zhu, B.; Inoue, Y. Prog Polym Sci 2004, 29, 1021.
23. Al-Najjar, M. M.; Hamid, S. H.; Hamad, E. Z. Polym Eng Sci 1996, 36, 2083.
24. Daniliuc, L.; David, C. Polymer 1996, 37, 5219.
25. McCrum, N. G.; Read, B. E.; Williams, G. Anelastic and Dielectric Effects in Polymeric Solids; Wiley: New York, 1967.
26. Boyd, R. H. Polymer 1985, 26, 323.
27. Bershtein, V. A.; Egorova, L. M.; Yakushev, P. N.; Pissis, P.; Sysel, P.; Brozova, L. J Polym Sci Part B: Polym Phys 2002, 40, 1056.
28. Vatalis, A. S.; Kanapitsas, A.; Delides, C. G.; Viras, K.; Pissis, P. J Appl Polym Sci 1999, 80, 1071.
29. Pissis, P.; Apekis, L.; Christodoulides, C.; Niaounakis, M.; Kyritsis, A.; Nedbal, J. J Polym Sci Part B: Polym Phys 1996, 34, 1529.
30. Donth, E. Relaxation and Thermodynamics in Polymers: Glass transition; Akademie: Berlin, 1992.
31. Angell, C. A. J Non-Cryst Solids 1991, 131/133, 13.
32. Lattimer, R. P.; Williams, R. C. J Anal Appl Pyrolysis 2002, 63, 85.
33. Herrera, M.; Matuschek, G.; Kettrup, A. Polym Degrad Stab 2002, 78, 323.
34. Kim, S.-S.; Kim, S. Chem Eng J 2004, 98, 53.
35. Faravelli, T.; Pinciroli, M.; Pisano, F.; Bozzano, G.; Dente, M.; Ranzi, E. J Anal Appl Pyrolysis 2001, 60, 103.
36. McNeill, I. C.; Liggat, J. J. Polym Degrad Stab 1992, 36, 291.
37. He, Y.; Zhu, B.; Inoue, Y. Prog Polym Sci 2004, 29, 1021.